Check for updates

# Machine learning in the search for new fundamental physics

*Georgia Karagiorgi*[1] ✉, *Gregor Kasieczka*[2] ✉, *Scott Kravitz*[3] ✉, *Benjamin Nachman*[3,4] ✉ *and David Shih*[5] ✉

Abstract | Compelling experimental evidence suggests the existence of new physics beyond the well-established and tested standard model of particle physics. Various current and upcoming experiments are searching for signatures of new physics. Despite the variety of approaches and theoretical models tested in these experiments, what they all have in common is the very large volume of complex data that they produce. This data challenge calls for powerful statistical methods. Machine learning has been in use in high-energy particle physics for well over a decade, but the rise of deep learning in the early 2010s has yielded a qualitative shift in terms of the scope and ambition of research. These modern machine learning developments are the focus of the present Review, which discusses methods and applications for new physics searches in the context of terrestrial high-energy physics experiments, including the Large Hadron Collider, rare event searches and neutrino experiments.

For several decades, the standard model (SM) of particle physics has provided a clear theoretical guide to experiments, resulting in an extensive search programme that culminated with the discovery of the Higgs boson[1,2]. Although the SM is now complete, there are key experimental observations that compel the community to expand the search efforts for new particles and forces of nature beyond the SM (BSM). For example, the existence of dark matter (DM) and dark energy is well established[3], as are the mass of neutrinos[4,5] and the baryon–antibaryon asymmetry in the Universe[6] — yet none of these observations are explained by the SM. Additionally, 'aesthetic' problems plague the SM, including the unexplained weak-scale mass of the Higgs boson, the existence of three generations of fermions, and the minuteness of the neutron dipole moment[7]. Current and near-future high-energy physics (HEP) experiments have the potential to shed light on all of these fundamental challenges by creating new particles in the laboratory, or by observing interactions of new particles with normal matter or with other new particles.

This great potential for discovery comes with considerable data challenges. New particle interactions are expected to be rare, and their signature could be only subtly different from the SM. This means that researchers must collect and sift through an immense amount of complex data to isolate potential BSM physics. Machine learning (ML) offers a powerful solution to this challenge. Deep learning techniques (used here to mean modern ML, with deep neural networks (NNs) and other advanced tools that contain (much) more than tens of thousands of tunable parameters) are well suited for analysing large amounts of data in many dimensions to find subtle patterns. Multivariate analysis has been commonplace in HEP for decades (for example, the TMVA 'toolkit')[8], but the latest tools will qualitatively extend the sensitivity to 'hypervariate analysis' whereby the entire phase space of available experimental information can be analysed holistically. These new tools also allow for new analysis strategies independent of the dimensionality (density estimation, variable-length inputs and so on).

In tandem with the growing data volume, a related challenge is the increasing need for efficient (in terms of computational time, power and resource utilization) and accurate data processing for high-throughput applications. Efforts to that end include the development and acceleration of deep learning-based processing algorithms on power-efficient hardware platforms[9].

In addition to the growing data challenge, there is also the compounding challenge of simulating expectations for what experiments may observe. HEP experiments rely heavily on simulations for all aspects of research, from experimental design all the way to data analysis. Built on a thorough understanding of the SM and the fundamental laws of nature, these simulations are extremely comprehensive and sophisticated, but they are still only an approximation to nature. It is therefore often necessary to combine simulations with information directly from data to improve simulation accuracy. The corresponding ML models must be robust against inaccuracies and be able to integrate uncertainties.

[1]*Department of Physics, Columbia University, New York, NY, USA.*

[2]*Institut für Experimentalphysik, Universität Hamburg, Hamburg, Germany.*

[3]*Physics Division, Lawrence Berkeley National Laboratory, Berkeley, CA, USA.*

[4]*Berkeley Institute for Data Science, University of California, Berkeley, CA, USA.*

[5]*NHETC, Department of Physics and Astronomy, Rutgers University, Piscataway, NJ, USA.*

✉*e-mail: georgia@nevis.columbia.edu; gregor.kasieczka@uni-hamburg.de; swkravitz@lbl.gov; bpnachman@lbl.gov; shih@physics.rutgers.edu*

https://doi.org/10.1038/s42254-022-00455-1

**Key points**

- There have been large and sustained developments of deep learning in high-energy physics over the past several years.
- Supervised machine learning methods are widely used to identify known particles and to design targeted searches for specific theories of new physics.
- Less-than-supervised machine learning methods are used to carry out searches that depend less on a specific signal model.
- Experiments such as those at the Large Hadron Collider, neutrino detectors and rare event searches for dark matter, despite having different technical requirements, also share similarities, and there is ground for cooperation to develop machine learning methods.
- Combining physics and new ideas from statistical learning will be crucial to analysing the large volumes of data to potentially uncover the fundamental structure of nature.

BSM physics can also be precisely simulated, and most searches are developed, optimized and interpreted in the context of a specific BSM model. It is not possible to test every model with a dedicated search, and even if this could be done, there would still be blind spots in the search programme. Here, again, ML and in particular unsupervised ML methods are starting to provide a complementary search strategy that is liberated from model dependence compared with traditional searches.

## Scope

This Review focuses on the applications of modern ML to the search for new fundamental physics. For ML applications to SM physics, see a previous review[10]; a living review of ML for particle physics[11] includes a more complete and continuously updated list of references. Here we only sample some early examples without attempting to be exhaustive. To keep the scope of this Review manageable, we focus on terrestrial experiments that directly probe BSM effects and that aim to elucidate the particle nature of BSM physics. This includes production of new, massive particles at the Large Hadron Collider (LHC), rare event searches — such as direct detection of DM — in the laboratory, and searches for weakly interacting particles such as sterile neutrinos. These three science frontiers (energy, rare event, neutrinos) have much in common, starting with their fundamental units of data: all three are 'event' based, where each event represents a (nearly) independent and identically distributed draw from an ensemble of physics processes (typically, particle interactions with other particles, or matter in a detector). Although the structure and format of recorded events can differ between these frontiers, a similar data pipeline is followed for all experiments.

The first step of the data pipeline is to record potentially interesting events with real-time or online algorithms (data acquisition). Then, various pattern recognition algorithms are used to reconstruct and calibrate the properties of recorded events (data reconstruction). Finally, certain events are selected based on their properties and used for statistical analyses (final data analysis). A parallel track also runs on simulation, where synthetic events are generated and then passed through these same steps. ML is actively being integrated into each of the three steps, with considerable innovation from HEP domain scientists to design custom solutions to the fields' unique challenges.

Below, we highlight advances from ML in all aspects of the data pipeline, with a focus on new particle searches. Although many ML-based reconstruction innovations are now being integrated into experimental workflows, data acquisition and final data analysis tools are not yet widely deployed, owing to the newness of the methods being developed, and the time it takes to turn them from proofs-of-concept into complete analyses. We note that the frontiers vary in how they have been using deep learning so far; we present the three frontiers with equal space, but this necessarily means that for the frontiers using more advanced deep learning at the moment, this Review is less specific and/or does not cover less sophisticated approaches in detail.

Although this Review is focused on direct searches for new particles, there are also many indirect searches in the form of SM measurements. Analyses probing small differences between the SM and the data are also increasingly using ML strategies for data corrections in the presence of BSM[12,13], effective field theory analysis[14–21], reinterpretation[22–24] and more[11].

## Machine learning basics

ML involves four or five components: input features $x \in \mathbb{X} = \mathbb{R}^N$, (sometimes) targets $y \in \mathbb{Y} = \mathbb{R}^M$, a model $f: \mathbb{R}^N \to \mathbb{R}^M$ with tunable parameters (where $N$ and $M$ are the dimensions of the inputs/targets, respectively), a loss functional $L[f]: \mathbb{X}^{\mathbb{Y}} \to \mathbb{R}$, and an optimization strategy. When targets (called labels) are available for each training example, the procedure is called supervised learning, otherwise the approach is less-than-supervised. If labels are present for only some of the examples this is called semi-supervised learning, whereas if labels are noisy the approach is weakly supervised learning. Lastly, if labels are not present at all, this is called unsupervised learning. In HEP, owing partially to quantum mechanics, it is often impossible to know the labels of individual examples from real data. However, simulations (using Monte Carlo methods) play a key role in the development and execution of searches for new particles, and it is usually possible with simulated data sets to have per-instance labels by examining the Monte Carlo truth record (internal history of particles generated).

For many applications, $N = \mathcal{O}(1)$ as the features are a fixed set built from the full phase space based on physical intuition. In this case, boosted decision trees (BDTs) and shallow NNs have long been the tools of choice for ML in HEP. Meanwhile, deep learning methods, such as NNs, are now able to readily process high-dimensional feature spaces where $N$ can be many thousand or more. $N$ may not be fixed for each data point because, for example, LHC proton–proton collision or neutrino/dark-matter interaction events naturally produce a variable number of particles.

### *Data representations*

The choice of how to represent the data (for example, four-vectors of every particle in the event, energies of calorimeter deposits) can play an important role in the design (architecture) of the deep learning algorithm, and can have a significant impact on its performance.

The most flexible and general architecture is that of the fully connected or dense neural network (DNN), where the features $x$ are simply flattened to a column vector, and fed to the DNN which is specified by the number of hidden layers, the number of nodes in each hidden layers, and so on. Often the humble DNN is sufficiently powerful for many applications in HEP. But fundamental physics events often respect various symmetries, which can be built into ML architectures to reduce the number of parameters and increase performance.

If $x$ can be represented as a fixed-size tensor with translational invariance across indices, then $f$ is usually a convolutional neural network (CNN)[25,26]. For example, it is often natural to represent fundamental physics events as images, with the pixel intensity given by the amount of energy deposited in a given detector region (such as a calorimeter cell). If a particular physics signature can register anywhere in the detector, then translational invariance is a good symmetry. The early applications of CNNs to particle physics[27,28] showed that CNNs can still be useful even if translational symmetry is broken from pre-processing (image centring). Studies of homogeneous detectors such as those common in neutrino physics were among the first to exploit the translational invariance of these methods[29].

Other architectures are well suited when $x$ has structure other than a translationally invariant tensor. If $x$ is a sequence, then recurrent neural networks (RNNs) are particularly effective[30,31]. Whereas CNNs share weights across space, RNNs share weights across time (location in the sequence). As sequences can vary in length, RNNs were the first tools for processing variable-dimensional features in HEP (for jet flavour tagging)[32]. When $x$ is a hierarchy of sequences (called a tree), then recursive neural networks can be used in a similar fashion to RNNs. Tree structures arise naturally in high-energy jet clustering and have been studied in that context to identify Lorentz-boosted $W$ bosons decaying into hadrons[33].

One challenge with image, sequence and tree representations of data is that they require a spatial or temporal order to the dimensions of $x$. Although this is often natural, in many cases there is no inherent order. For example, the particles of the same type produced in collider and fixed-target experiments are indistinguishable owing to quantum mechanics. It is possible to impose an order (such as sort by energy), but this does not necessarily reflect the underlying physics processes or associations. There are now multiple architectures that can process variable-length and permutation-invariant sets. A neural network $f$ is invariant under the operation of a group $G$ if $f(g(x)) = f(x)$ for all $g \in G$; the network is equivariant if $f(g(x)) = g(f(x))$. See other work[34–37] for examples of equivariant networks in HEP. One example is deep sets[38], adapted to particle physics as the Particle Flow Network[39] for instance. In this framework, NNs are decomposed into two parts: a network that embeds each of the $N/n$ components of $x_i$ into a latent space $\Phi : \mathbb{R}^n \to \mathbb{R}^k$ (where $n$ and $k$ are the input and latent dimensions, respectively) and a second network $F$ that processes the sum over latent space vectors: $f(x) = F(\Sigma_i \Phi(x_i))$. A second permutation-invariant architecture is the graph neural network (applied in particle physics[40–46] and reviewed previously[47]), which makes use of locality in the passage of information between nodes of the graph and layers of the network.

### *Machine learning tasks*

ML tasks are categorized by the learning target, $y$, if they are available. When $y$ is discrete and finite, the task is called classification and the typical loss functional is the cross entropy: $L[f] = \Sigma_i \Sigma_j \mathbb{I}[y_i = i] \log(f_j(x_i))$ for classes $j$, indicator function $\mathbb{I}$, and $\Sigma_j f_j = 1$. For continuous (or discrete and infinite) $y$, the task is called regression and a common loss functional is the mean squared error: $L[f] = \Sigma_i (f(x_i) - y_i)^2$. Other loss functionals correspond to different learning targets (mean, median, mode and so on); see elsewhere[48] for details in the context of HEP. As described earlier, both these classification and regression tasks are supervised, since each data point $x_i$ comes with a label $y_i$.

At the other extreme is unsupervised learning which proceeds without any labels. Such approaches are typically designed to learn implicitly or explicitly the data probability density $p(x)$. This can be useful for various tasks including generative modelling and anomaly detection. The three standard approaches to unsupervised deep learning are generative adversarial networks (GANs)[49,50], (variational) autoencoders (VAEs)[51,52] and normalizing flows (NFs)[53,54], studied in HEP in REFS[55,56], REFS[57–60] and REFS[61–65], respectively. Each of these methods (although for autoencoders, this is only true for variational architectures) learns to map a random variable $Z \in \mathbb{R}^k$ with a known probability density to the data. For GANs, a second network $h$ is simultaneously trained to distinguish $f(Z)$ from $X$; when that network performs poorly, then $f$ is a good model of the data. For VAEs, $f$ is the decoder of a two-network encoder–decoder setup. The data are mapped from the data space into the latent space via the encoder and then back to the data space via the decoder, trying to preserve the data distribution and statistical properties of the latent space. A normalizing flow is a series of invertible functions $f_i$ with tractable Jacobians in order to change $Z$ into $X$: $p_f(f(z)) = p(z) \prod_i |\partial f_{i+1}^{-1} / f_i|$ for $f_0 = z$. NFs are optimized by maximizing the likelihood of the data: $L[f] = \log p_f$.

Finally, there is a spectrum of less-than-supervised tasks between fully supervised and fully unsupervised techniques. In general, these use a mix of information from data and from simulation. Semi-supervised methods have labels available for some but not all data. Note that such a categorization is not unique; see elsewhere[66] for an alternative way of defining weak supervision. We follow the established usage in applications of ML for particle physics. Weakly supervised methods have labels for all data, but each label is noisy. These approaches have been studied in HEP[67–70]. For example, if a set of events is known to be composed of two classes and the class proportions are $p_0$ and $p_1 = 1 - p_0$, then randomly assigning the label 0 with probability $p_0$ would constitute noisy labels. This is the assumption that underlies 'learning from label proportions'[67]. Learning may still be possible even if the proportions are not known, as is the case in 'classification without labels'[68].

## Machine learning searches for new physics

In this section, we review the current state of the art in methods for direct new physics searches at particle detectors. Many of the ideas presented here are still at the proof-of-concept stage; in the next section we describe the status of methods that have been applied to actual data.

A search for new physics requires two essential components. The first is a method for achieving signal sensitivity by selecting events that preferentially contain new physics, removing as many of the (generally far more numerous) SM background events as possible. The second is the careful and precise estimation of the SM background. Events in data that have passed a selection are compared to a prediction of the SM background for the same selection. If the number of events or their distribution in some observable is inconsistent between data and SM background prediction, there is evidence for new phenomena. If the data are consistent with a particular BSM theory, then that model's parameters can be estimated; otherwise, limits are placed on the new particle parameters. Usually, both the 'discovery' and 'limit-setting' modes are run in parallel for a given BSM search.

The role of SM and BSM modelling (often via simulations) in both achieving signal sensitivity and estimating the SM background can be used to categorize different search strategies (FIG. 1). Note that this categorization does not imply a ranking; to the right and up on these graphs does not mean better. On the contrary, we will need a diverse set of strategies to achieve broad and deep coverage of BSM possibilities. At present, most searches achieve signal sensitivity in a simulation-based and model-specific way. These searches begin by positing the existence of new particles with particular physics-theorized parameters (masses, couplings and so on). Given such a model, simulations can be used to predict what the new phenomena would look like in a detector. Combined with simulations of the SM, and often augmented with data-driven approaches for background estimation, a search strategy can be devised that would reject SM processes and enhance the presence of new particle processes in a given set of data. Increasingly, searches use modern ML to train supervised classifiers for this purpose, and use them in all stages of a data pipeline to enhance sensitivity to predictable signatures of new physics.

A growing number of methods that make use of less-than-supervised ML techniques are being proposed for more model-agnostic and simulation-independent new physics searches. (A series of non-ML semi-supervised searches has been conducted over recent decades at DØ[71–74], H1[75,76], ALEPH[77], CDF[78–80], CMS[81–84] and ATLAS[85–87]. All of these searches share essentially the same approach: they compared (many) histograms of data to histograms of SM simulations and looked for discrepancies). For example, various methods have been proposed that use the data itself to enhance the signal sensitivity. Data are unlabelled by construction, and so any approach of this type is necessarily less-than-supervised.

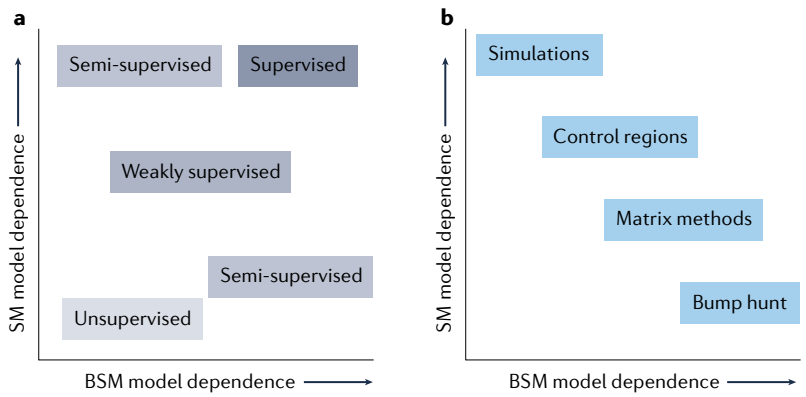


Fig. 1 | **Illustration of the landscape of model dependence. a** | Landscape for achieving signal sensitivity. **b** | Landscape for calibrating the standard model (SM) background. Supervision refers to the type of label information available during training. Supervised searches use simulation (labelled by construction) for the signal and the SM background. Semi-supervised searches use data (unlabelled by construction) for either the background or the signal-sensitive sample. Weakly supervised searches have labels for every example, but the labels are noisy. Finally, unsupervised methods do not use any label information. In rare cases with relatively simple processes, SM simulations can be used directly to estimate the background. Most of the time, a combination of data and simulations is used to estimate the SM background. The control region method uses an auxiliary measurement in a signal-poor region to constrain the simulation. Various matrix methods (such as the ABCD method) use two independent features that are both signal-sensitive to predict the background. Bump hunts assume that the signal is localized in one dimension (often an invariant mass) where a sideband fit can be used to predict the background in the resonant region. BSM, beyond standard model. Figure adapted from REF.[65], under a Creative Commons licence CC BY 4.0.

### *Signal model-driven or fully supervised searches*

Using simulations of the SM and new particles, fully supervised classifiers are trained to distinguish pure signal from pure background. The resulting classifiers are then applied to data and used to enhance the presence of a potential signal. There are generally two ways to train these supervised classifiers. One approach is to train using all information in an event; another is to train using particular objects. For example, a new heavy particle $X$ produced at a collider decaying into a pair of Higgs bosons with $m_X \gg m_h$ will result in two collimated sprays of particles (called jets), one for each Higgs boson. One option is that a classifier could be trained using the full event to exploit the properties of the $X$ production and decay. A second option is that a dedicated 'tagger' for classifying Lorentz-boosted Higgs boson jets from generic quark and gluon jets could be constructed. Particle taggers can then be combined with other tools to form an event-level classifier. There are advantages and disadvantages for each approach. A key advantage of object tagging is that calibrations (with uncertainties) can be derived in one setting and applied in many other cases. This is not possible with event-level tagging. The sections below discuss signal sensitivity (object tagging and event-level classification) and background estimation for supervised searches.

***Object tagging.*** Jet tagging has driven much of the innovation in signal classification, owing to their complexity and ubiquity at HEP colliders. A jet can be composed of tens to hundreds of particles, and each particle has a four-momentum and other attributes such as electric

charge. As a result, jets exist in a high- and variable-dimensional space, and deep learning has been used to study them as images, sequences, trees, sets and graphs. Bottom quark jet tagging has a long history of using ML with low-level experimental inputs and top quark jet tagging has become a benchmark task for studying new methods, as described in the community report[88]. ML has also been used extensively to tag single particles such as electrons, muons and pions in collider, fixed-target and neutrino experiments[89]. When measured by multiple, segmented detectors, these objects can be represented by many features, and ML can be a powerful tool for a variety of classification and regression tasks. Examples of tagging for composite and single objects in an experimental context are given in the next section.

***Event classification.*** Numerous event-level classifiers have been used for enhancing signal sensitivity across HEP. BDTs are particularly common. An early study[90] compared deep learning with more traditional shallow learning methods. A conclusion from this study that has since been repeated many times is that deep learning methods can process low-level inputs (particle four-vectors) and achieve comparable or superior performance to shallow methods that take as input physics-engineered high-level features. The move from $\mathcal{O}(10)$ features to many hundreds or thousands of input features was reported in papers[29,91] that represented entire neutrino/collider events as images and processed them using CNNs. Similar to the earlier studies, it was found that deep learning on low-level inputs was able to exceed the sensitivity of standard approaches and did not improve when hand-crafted observables constructed from low-level inputs were provided to the NNs.

***Background estimation.*** ML has been proposed to enhance each of the background estimation strategies highlighted in FIG. 1. Strategies based completely on simulation can be optimized end-to-end in an inference-aware approach[92–99] such that the learning knows about the final test statistic and hypothesis test. Hybrid methods that use auxiliary measurements to constrain the simulation can be made uncertainty-aware[14–17,100–105] by incorporating aspects of the statistical and systematic uncertainty during training. Simulation corrections (called domain adaptation in ML) can be derived from auxiliary measurements in many dimensions by ML methods as well[106–112]. Matrix methods rely on the independence of features, which can either be assumed physically and then combined with machine learning[113] or enforced with ML[114,115]. Bump hunts can be enhanced with ML, but they must not sculpt localized features. This can be achieved with decorrelation methods[114,116–132], which automatically ensure that classifiers have a controlled dependence on the resonant feature(s). A well-studied case is when there is no dependence (independence) on the resonant feature. In some cases (such as the bump hunt), decorrelation is not needed — all that is required is that the classifier is monotonic with the resonant feature[129]. Decorrelation derived in simulation may also not directly translate to data, which is a source of systematic uncertainty. Decorrelation tools have also been proposed to reduce uncertainties[117,126], although this should be approached with caution[133]. There is also a connection to the ML field of fairness, which endeavours to make classifiers equal (invariant) or equitable across populations[134,135]. ML has also been studied for other aspects of bump hunts, including highly flexible background fits[136–138].

### *Less-than-supervised searches*

Supervised searches are often constructed as simple hypothesis tests, where the presence of signal is one hypothesis and the other is the SM-only hypothesis. When the signal hypothesis is rejected, then the hypothesized model is excluded, typically at 90% or 95% confidence. In the absence of nuisance parameters, the optimal test statistic for this hypothesis is the likelihood ratio $p_{\mathrm{SM+BSM}}(x)/p_{\mathrm{SM}}(x)$ (REF.[139]). Optimal in this context means that for a fixed probability of rejecting the given hypothesis when it is true (level), the probability for rejecting the given hypothesis when the alternative is true (power) is maximized with the likelihood ratio test statistic. In the presence of nuisance parameters, there is no uniformly best test statistic, but the likelihood ratio is still very powerful and widely used. Note that any test statistic that is a monotonic function of the likelihood ratio will have the same statistical properties.

Less-than-supervised searches do not have a particular signal hypothesis. In this case, it is not possible to construct a test statistic that is optimal for all potential signals. However, it is still possible to develop methods for discovering new physics signatures that are statistically motivated. Unsupervised searches typically target events with low $p_{\mathrm{SM}}$. Weakly and semi-supervised methods use some label information and are therefore able to construct alternative likelihood ratio statistics such as $p_{\mathrm{data}}(x)/p_{\mathrm{SM}}(x)$. This test statistic is optimal for a data-versus-background hypothesis test, and when ML methods are trained with samples drawn from the exact $p_{\mathrm{SM}}$, the test statistic is sometimes called the idealized anomaly detector.

Most less-than-supervised searches in HEP differ from the typical anomaly detection setting in industry because $p_{\mathrm{SM}}$ is usually not zero. No single event can be labelled as signal with certainty, and so HEP often targets group or collective anomalies as opposed to point or off-manifold anomalies that are common elsewhere. Many examples of less-than-supervised methods can be additionally found in the recent LHC Olympics and Dark Machines community challenge reports[140,141].

***Unsupervised.*** The strategy of unsupervised anomaly detection methods is to find data points that are far from the bulk of the background. A common approach is the autoencoder network architecture[142]. Here, a pair of networks form a lossy compression algorithm. One network (the encoder) maps data into a latent space representation, and a second network (the decoder) maps from this latent space back to data. These networks are trained to minimize a loss function such as the absolute difference between input data and decoder output. By limiting the capacity of this transformation, the autoencoder can

be prevented from learning the identity function and instead identify relevant features of the data. If trained on data dominated by a background process, an autoencoder accordingly will learn to minimize the loss for it while returning a higher loss for previously unseen signal data.

Since the initial proposals of using autoencoders for anomaly detection[58–60], a number of improvements and modifications have been suggested. An important observation is that autoencoders can be biased by the relative complexity of anomalous and background data, potentially leading to outliers with a lower loss than the background[143–146]. As the latent space in VAEs[51,52] is optimized to follow a known distribution for backgrounds, it can also be used as anomaly score[147,148].

Beyond the autoencoder family, a number of other unsupervised approaches based on support vectors[149], latent space Dirichlet analysis (LDA)[150,151], clustering[152] and GANs[153] have been investigated.

***Weakly and semi-supervised.*** In contrast to unsupervised searches, weakly and semi-supervised searches use some label information to inform the training. This can result in an improved sensitivity for BSM particles, at the cost of additional assumptions[154,155]. The aspect that distinguishes weakly supervised learning and semi-supervised learning is the fidelity of the labels. Weakly supervised learning uses noisy labels whereas semi-supervised learning use noiseless labels, but only for a subset of the training examples.

In particle physics, the usual application of weak supervision is to isolate two sets of data (call them A and $B$) that are each composed of the same two classes 1 and 0 (1 for signal and 0 for background). The probability density of the mixtures A and $B$ are then given by $p_A = \varepsilon_A p_1 + (1-\varepsilon_A)p_0$ and $p_B = \varepsilon_B p_1 + (1-\varepsilon_B)p_0$, for some unknown signal fractions $\varepsilon$A and $\varepsilon_B$. If $\varepsilon_A > \varepsilon_B$, then mixture A is given the noisy label of signal-like and mixture $B$ is given the noisy label of background-like. If a classifier is trained using these noisy labels, it will learn a function monotonically related to $p_A/p_B$ that is itself monotonically related to $p_1/p_0$ and thus optimal for the target task.

This weakly supervised approach works well only when the 1 and 0 classes in A and $B$ are statistically identical. Otherwise, the classifier will be distracted by differences between A and $B$ that are unrelated to the signal. This means that whatever features are used to construct A and $B$ must not significantly distort the features used for classification. Note that this imposes a mild assumption on the signal, as this independence must be true for both classes. One widely studied setting where this applies is resonance searches. Such searches are defined by a feature $m$ (often an invariant mass) that is resonant for a potential signal and without localized features for the background. The 'classification without labels' approach[156,157] proposed using a region near the potential signal to construct $A$ and using a sideband region to define $B$. Another option is to build $B$ using pure[158–160] or data-augmented[161,162] simulation, which is composed of only the 0 class by construction. Simulations can also be used to add signal-like labels for $A$[163,164]. Hybrid approaches have also been proposed that use parameterized density estimation from the sideband to estimate the background density in the signal region[65,165,166] or autoencoders to learn the noisy labels in the first place[154]. Many of these methods are also naturally robust to correlations between $m$ and the classification features.

## Frontier highlights

This section presents the current status of ML in the energy, neutrino and rare event frontiers. Events at energy frontier experiments occur at the same point in space (centre of the detector) at a fixed frequency and directly probe the highest energies with terrestrial experiments. The current energy frontier experiments are at the LHC. Events in neutrino experiments are usually time-synchronous with the reactor or accelerator neutrino source, but can occur anywhere within the detector. The space and time of events in rare event experiments are not controlled by the experimenters. These searches for DM direct detection, astrophysical neutrinos and as well as other weakly interacting phenomena typically require large detectors built deep underground. This section highlights ML applications across all three steps of the data pipeline, including data acquisition, data reconstruction and final data analysis.

### *Energy frontier*

The goal of direct new physics searches at the LHC is to test the SM at the energy frontier, by producing new BSM particles, and then endeavouring to detect their distinctive signatures (for instance through their decays to SM particles) over the SM background. Examples of new physics scenarios searched for at the LHC include supersymmetry, extra dimensions, black holes, DM, new generations of quarks and leptons, and new fundamental force carriers ($Z'$s).

ML has found widespread use across LHC experiments. At the lowest levels, ML is used for detector calibrations, data acquisition, pattern recognition, denoising, particle identification and detector simulation. At the level of individual analyses, ML is used for background estimation and for constructing final analysis discriminants. Below, we highlight a few examples from these areas.

***Data acquisition.*** One of the key challenges at the LHC is the extremely high data rate, with collisions happening at 40 MHz and each event requiring $\mathcal{O}$(MB) of memory. It is not possible to write every event to disk, so considerable online processing is required. The ATLAS and CMS experiments use a two-stage processing to discard more than 99.99% of events and reduce the data rate to 1 kHz. To achieve the needed low latency, the first stage (termed level-1-trigger, L1T) is implemented using field-programmable gate array (FPGA) hardware whereas a second stage (termed high-level-trigger, HLT) runs on computer hardware such as CPUs or GPUs. So far, shallow ML has been used in the trigger. For example, CMS used BDTs to improve the muon momentum resolution at L1T[167] via look-up tables on FPGAs storing the pre-computed output values for different inputs. Similarly, LHCb used an efficient BDT

implementation — termed bonsai BDT[168] — in the trigger[169]. For upcoming data-taking periods, plans exist to include deep networks at L1T[9,170–175], to further improve the selection efficiency.

A particularly interesting strategy of removing the first hardware stage of the trigger and processing all events by a software trigger stage running at 30 MHz is considered by the LHCb experiment[176]. Using the parallelization capabilities of GPU-hardware allows track reconstruction to be executed and physics-based selections to be made at the full input rate of 30 MHz, corresponding to 40 Tbit $s^{-1}$ of raw data and thereby reducing the input to subsequent selection stages by a factor of 20–40 (REF.[177]). The presence of GPU-hardware also enables the relatively simple adaptation of highly accurate ML algorithms in the trigger to further improve selection efficiency.

Deep generative models are now being deployed for creating large synthetic data sets that will be used for all aspects of downstream inference tasks[57,178–180].

***Object tagging.*** Identifying known SM particles to enrich samples that include a specific physics process of interest is common practice at the LHC, and ML-based taggers are studied — and in many cases deployed — for essentially all such object tagging tasks. One example of a single-object tagger is tagging jets originating from a *b*-quark (*b*-tagging). The DL1 algorithm used by the ATLAS collaboration[181] is a fully connected DNN achieving a light-flavour (*u*/*d*/*s* quark and gluon jets) false-positive rate of 1/390 while retaining 70% true positive rate (efficiency) for true *b*-quark jets, greatly outperforming simpler approaches. These methods are widely used, with a large fraction of analyses requiring at least some kind of flavour information. At the same time, architectures tailored to using low-level properties and symmetries of data promise further gains in performance[182,183].

A similar situation exists for more complex signals. Considering detector activities in a larger geometrical region using 'large-radius jets'[184,185] allows for the identification of hadronically decaying, Lorentz-boosted heavy resonances such as *W*, *Z* or Higgs bosons and top quarks. For example, see an overview[186] of tagging methods considered by the CMS collaboration. Again, such standard taggers are used across a large number of applications[187–190] to enrich the relative fraction of the desired particle or to design signal-regions for searches.

Both for narrow and large jets, these methods can be calibrated and scale factors can be provided by comparing recorded data and Monte Carlo simulations[181,186,191–193]. Finally, taggers are also developed for hypothetical, unobserved, signal particles. In this case, training has to rely on simulation, and calibration in data is only possible for backgrounds[194], putting an additional emphasis on robust background estimation techniques.

***Background estimation.*** Decorrelation strategies are widely used by ATLAS, CMS and LHCb to enable resonance searches with ML; see elsewhere for performance studies[124,186,195] and for recent examples of physics results[196–198]. A growing number of searches using control region methods employ ML to perform high-dimensional reweighting to better match the background data in signal-sensitive regions[199,200]. The mitigation of data/simulation differences can also be part of the classifier training directly[194].

***Final analysis discriminants.*** Shallow, fully supervised ML (for example BDTs) is ubiquitous in searches at the LHC. For example, ATLAS and CMS have published over 600 papers searching for new particles, and the TMVA multivariate analysis package[8] is cited in over 10% of them. This does not include the analyses that use per-object ML-based classifiers (described above), which are likely to be a large fraction of all searches. A growing number of searches are exploiting deep learning for the final analysis setup, using a variety of combinations of signal sensitivity and background specificity approaches highlighted in FIG. 1.

The most common applications of deep learning to event-level analysis use supervised methods. For example, the recent ATLAS search using multiple charged leptons[201] is fully supervised, and given the precisely known multilepton final state, simulations are used directly for the background estimation. A search by CMS in the $bb\tau\tau$ final state uses an event-level, supervised classifier that is mostly calibrated using a control region method[202]. An example of a search using matrix methods for the background estimation is the recent ATLAS search for exotic Higgs boson decay to *a Z* boson and a light pseudoscalar[203]. To maintain sensitivity across pseudoscalar masses, a classification network is combined with a mass regression network before estimating the background using the ABCD method[114]. There are many resonance searches that use supervised learning, but they are all currently using ML through object classifiers.

Although there have been many proposed less-than-supervised searches, few were put into practice, owing to the time required to perform a complete data analysis. There is a tradition of semi-supervised analyses that use signal simulations and control region data to build analysis discriminants. A recent result of this type using modern ML is the diphoton search from ATLAS[204] that uses XGBoost[205]. The first weakly supervised analysis was performed by ATLAS in the dijet final state, using the 'classification without labels' protocol[198]. Despite this initial result only using two features, it was still able to extend the sensitivity of inclusive searches by automatically identifying anomalous regions of phase space.

Whereas this section has focused on the LHC, modern ML tools are also being applied at Belle II (for example, in tracking)[206], and older ML algorithms have a long history at previous colliders and will be essential for the physics program of future colliders.

### *Neutrino experiments*

The discovery of neutrino masses (through the observation of their flavour oscillation) is not explained by the SM. Current searches in neutrino physics seek to understand the origin of neutrino masses and uncover

deviations from the three-neutrino paradigm, for example the existence of light sterile neutrinos[207,208], new fundamental force mediators[209,210], extra dimensions[211], Lorentz and charge–parity–time (CPT) symmetry violation[212], or non-standard interactions of neutrinos with matter[213,214]. A key requirement for these analyses is the classification of the interacting neutrino flavour through identifying interaction final states, which is used to probe deviations to the standard neutrino oscillation picture. Identifying the final state objects is also important for a broad set of analyses exploring neutrinos as a portal to DM physics. The phenomenology of these models often predicts non-standard final state objects such as long-lived particle decays to fermion–antifermion pairs[209,210]. Therefore, methods similar to object tagging for colliders are of growing interest and use, particularly for detectors with high spatial and calorimetric resolution.

With the need for increased precision, use of ML has been growing in neutrino experiments, through all stages of the data pipeline. Within the past five years, deep learning algorithms have become increasingly popular and have enabled large improvements in performance and physics reach compared with traditional methods. Deep learning applications now span the full extent of data processing for neutrino experiments, including data acquisition[215–218], final data analysis[219,220] and in particular data reconstruction[221–223], owing to the increasing use of large, high-resolution tracking calorimeters as neutrino detectors.

Compared with collider experiments, neutrino detectors usually comprise a large and homogeneous target where neutrino interactions can occur uniformly, leading to interaction signals that are translationally invariant. The features of interest are topological characteristics of illuminated pixels in a fixed segmented (2D or 3D) geometry, with spatially and temporally connected pixels correlating to a specific particle 'track' — the shape and length of the track, and the pixel intensity being indicative of the particle type and kinematic properties. As such, CNNs and other deep learning algorithms associated with computer vision have found strong relevance and thus become a particularly common and important tool in neutrino experiments[10]. An early demonstration[29] of CNNs applied to neutrino event classification based on their topology without the need for detailed reconstruction showed improved physics performance over traditional algorithms for the case of the NO$\nu$A experiment[224]. A comprehensive overview of ML in neutrino experiments is provided elsewhere[225]; the subsequent paragraphs highlight some of the more recent advances.

***Image recognition.*** A detector technology ideally suited for computer vision applications in neutrino physics is that of liquid argon time projection chambers (LArTPCs) — used by the future DUNE[226], current MicroBooNE[227] and upcoming SBN[228] experiments. These detectors function as stereoscopic image streaming devices, offering the possibility of direct application of image recognition at as early as the data acquisition stage. For the time being, however, applications of deep learning algorithms for these experiments have predominantly been focused on data reconstruction and final analysis tasks.

The DUNE collaboration is exploring the use of CNNs for neutrino interaction classification that allows for the simultaneous identification and classification of neutrino interaction final states and neutrino interaction type[229], while kinematics reconstruction with the use of 2D and 3D regression CNNs has been proposed[230]. MicroBooNE was among the first to demonstrate the successful use and advantages of CNNs for classifying signal versus background images, where signal images contain particles produced by a neutrino interaction[231]. Moving more toward the implementation of deep learning algorithms for reconstruction tasks rather than end-user analysis tasks, MicroBooNE has further demonstrated multiparticle type identification[89,231], as well as pixel-level object prediction[232] through a successful application of a UNet-style[233] CNN architecture and semantic segmentation techniques to LArTPC neutrino data. In an effort to minimize the computational needs for CNN applications to (particularly sparse) LArTPC data analysis, MicroBooNE has also demonstrated the use of semantic segmentation with a sparse CNN for event reconstruction[234]. This was motivated by previous work[235] that proposed a spatially sparse, UResNet-style architecture for particle-wise segmentation labels for LArTPC-like data sets[235]. SBN's near detector (SBND) has also applied a UResNet network for cosmic background removal[236], demonstrating scalability of larger CNNs for pixel-level signal-background rejection task with larger images[236]. The technique has also been used by MicroBooNE as part of the experiment's flagship BSM physics search[234].

More recently, a multitask, end-to-end optimization of a full data reconstruction chain for imaging detectors using sparse CNN and graph neural networks was demonstrated[237]. This chain consists of multiple neural network modules where each module performs a traditional data reconstruction task (such as clustering of pixels, particle type and momentum estimation, reconstruction of a particle flow, and hierarchy among parents and children)[235,238–240], and it is being integrated into DUNE's near-detector analysis and more experiments of this class[241].

Beyond the LArTPC experiments, additional pioneering applications of deep learning have exploited the unique detector geometry, working principle or raw data structure of a given experiment. For example, the NO$\nu$A detector's 2D imaging working principle has also prompted the development and use of a CNN for neutrino event identification and reconstruction[242], combining two orthogonal visual projections of given neutrino interactions in the detector and allowing the network to learn from independent 2D depictions of 3D energy depositions in neutrino interactions. The KamLAND-Zen detector, which is a roughly spherical detector, has made use of spherical CNNs for their physics analyses[243]. MINERvA has adapted CNNs with the use of domain adversarial neural networks as a way of mitigating unknown biases in the training inputs[112].

Finally, Daya-Bay, in one of the first demonstrations of unsupervised DNNs for pattern recognition, has demonstrated the use of dimensionality reduction as a method for interpreting features extracted by a CNN used in separating neutrino interactions from noise in their detector[244].

A unique case of deep learning reconstruction applications is that of the IceCube experiment, whose non-uniform detector configuration makes CNNs less fitted for the job. As such, IceCube has turned to the application of graph NNs, which are capable of dealing with irregular data geometries and sizes more effectively, finding significant improvement in physics performance over traditional algorithms[245,246].

***Data acquisition.*** With the use of increasingly large neutrino interaction target volumes and finer readout segmentation, data challenges for neutrino experiments begin to approach those of current collider experiments. For example, DUNE's multiple far detectors[247] will each generate raw data rates of several terabytes per second, and plan to be operated for at least a decade, requiring also 100% live-time (online and able to record data) in order to be sensitive to neutrinos from nearby supernova bursts or other stochastic BSM signals. With ML becoming increasingly common in neutrino experiments, the community is further steering its attention toward hardware acceleration of ML-based inference. GPU-accelerated ML inference as a service for computing in neutrino experiments is discussed elsewhere[248]; new developments are also targeting GPU- or FPGA-based acceleration for use of ML algorithms such as 1D or 2D CNNs in real-time or online processing of raw LArTPC data at the data acquisition and trigger level[215–217].

### Rare event searches

The primary goal of DM direct detection and neutrinoless double beta decay ($0\nu\beta\beta$) experiments is the observation of BSM processes, most commonly in the form of the scattering of weakly interacting massive particles or $0\nu\beta\beta$ via light Majorana neutrino exchange, respectively. Although ML in such searches is not as prevalent as in collider physics or neutrino experiments, perhaps owing in part to its particular sensitivity to mismodelling at the few-event level, its use has grown in recent years. At present, applications primarily consist of methods to improve either event reconstruction or signal/background discrimination.

***Shallow discriminators.*** Relatively simple methods such as BDTs remain popular, probably owing to their robustness and ease of use. BDTs have been used for the effective removal of rare backgrounds in xenon DM detectors such as LUX[249–251] and XENON1T[252], using high-level engineered features as inputs and applying a threshold on the output prior to future stages of analysis. Similar approaches have been used to remove noise pulses in solid-state DM detectors such as SuperCDMS[253] and COSINE-100 (REF.[254]). In the EXO-200 $0\nu\beta\beta$ experiment, this approach was taken a step further by combining the BDT output with other variables such as measured energy in the final 2D fit[255–257].

***Time series analysis.*** ML has also been harnessed for more complete analysis of time-series data (waveforms). More accurate extraction of pulse parameters, such as height and start time, has been demonstrated in solid-state detectors using principal component analysis (PCA)[258], CNNs and RNNs[259], while efficient (low-dimension) summaries of pulse shape have been achieved with BDTs[249] and convolutional autoencoders[260]. Background discrimination via pulse shape has shown promise, using either fully connected NNs or CNNs for bubble chamber DM experiments such as PICO[261,262], germanium neutrinoless double beta decay detectors[260], and cryogenic calcium tungstate DM detectors such as CRESST[263].

***Image recognition.*** Drawing on successful image recognition techniques in industry and neutrino experiments[231], rare event searches have implemented 2D CNNs to take full advantage of spatial (or spatio-temporal) information using light and charge detector hit patterns. This approach is particularly effective at topological signal/background discrimination in Xe time projection chambers (TPCs) for $0\nu\beta\beta$[264], including NEXT[265,266], nEXO[267,268], and PandaX-III[269], as well as the KamLAND-Zen $0\nu\beta\beta$ scintillator experiment[270] and even nuclear emulsion DM searches[271]. Two-dimensional detector hit patterns have also been used directly as inputs to CNNs, fully connected networks or Bayesian optimization methods[272] for more precise position reconstruction in noble element TPCs, such as EXO-200[273], XENON1T[274] and the Ar-based DarkSide DM experiments[275,276].

***Less-than-supervised searches.*** A common theme across rare event search experiments is the desire for reduced reliance on simulations, through fully data-driven training, semi-supervised or unsupervised learning approaches. Xe TPC experiments such as EXO-200 and LUX have trained ML models to better reconstruct events with either a missing charge or light signal, using data events with both present to provide labels for supervised training, after reweighting to reduce reliance on features exclusive to the original training domain such as its energy spectrum[249,273]. Imperfect labels from the selection of data events with unique signatures such as gamma escape peaks can be used to better identify single and multiple scatter events in germanium detectors[260]. Similarly, the Project 8 neutrino mass measurement experiment uses labels from calibration data events with known particle energy to classify tracks in frequency versus time spectrograms in cases where the energy is not as well constrained[277]. Supplementing simulated events with unlabelled data events, using confident network predictions as truth labels in subsequent training iterations, has been shown to boost performance in PICO[261,262]; in NEXT, features extracted through convolutional layers were found to agree more closely in simulations and data when augmenting training events by repeating them after physics-invariant transformations such as rotation[266]. Fully unsupervised methods, such as tSNE, PCA and autoencoders, have been successfully used to separate unwanted backgrounds through clustering in CRESST[259].

In many cases, the choice of representation of the data seems to have a greater effect on the results than the algorithm or architecture. PICO has observed improved particle discrimination from a simple fully connected network applied to the first few components of Fourier space data than a CNN in the time domain[261]. EXO-200 sees minimal improvement in discrimination when using a CNN classifier over a BDT with engineered features[257], while DarkSide-20k achieves improved performance using a fully connected network over a CNN[275]. In contrast, initial training of a convolutional autoencoder followed by training a fully connected network on its encoded latent space has shown good results in germanium[260], suggesting that separating the tasks of representation and classification may be more robust.

In the near future, an increased emphasis on extracting physical insights from unsupervised methods, careful quantification of uncertainties, and clever construction of training sets to reduce domain discrepancies will be crucial to taking full advantage of the benefits of deep learning in rare event searches.

## Challenges and opportunities

The development and deployment of ML methods in the search for new fundamental physics is becoming urgent given the dearth of evidence from traditional methods. New particles may be discoverable with existing and near-future experiments, but we may need to explore the data in its natural high dimensionality and to reduce the model dependence in order to uncover new phenomena. New methods are being developed at a rapid rate (inside and outside experimental collaborations), and we are starting to see many innovative applications to both data processing and data analysis.

The application of ML in fundamental physics has unique challenges that may not be solved by industry. Physicists are typically looking for ultra-rare and subtle deviations from the SM. Furthermore, it is often the case that no one datum is uniquely anomalous — only in the context of many examples can one build statistical evidence for a discovery. At the same time, it will also be essential to integrate state-of-the-art deep learning tools such as TensorFlow[278] and PyTorch[279] into analysis workflows to make the best use of new techniques. There are also serious computing challenges associated with training and inference. For example, the BSM exclusion limits in REF.[198] required training 20,000 NNs. This is because the event selection depends on the data and the data changes whenever a different amount of signal is injected. Especially for less-than-supervised searches, a radically new approach to data preservation and analysis reinterpretation will be required.

Astronomy and cosmology also offer unique and powerful windows into many types of BSM physics (such as DM, dark energy, baryogenesis, axions). These fields also generate enormous and complex data sets, with ongoing and upcoming observatories such as Gaia[280], the Laser Interferometer Gravitational-Wave Observatory[281], the Vera C. Rubin Observatory[282] and the Square Kilometer Array[283]. Much effort is already being invested in applying ML methods to accelerate data analysis and discovery in these fields; see elsewhere[284] for a comprehensive list of ML applications to cosmology. The connections between these areas and particle physics will be extremely interesting and important to explore.

Although many of the challenges associated with ML are technical, a new community mindset will also be required to take full advantage of the new tools. How can we make discoveries using representations we cannot easily visualize or understand? Forging physics with statistical learning provides a new path forward toward robust, sensitive and reliable methods for uncovering the fundamental structure of nature.

Published online 19 May 2022


1. Aad, G. et al. Observation of a new particle in the search for the standard model Higgs boson with the ATLAS detector at the LHC. *Phys. Lett. B* **716**, 1–29 (2012).
2. Chatrchyan, S. et al. Observation of a new boson at a mass of 125 GeV with the CMS experiment at the LHC. *Phys. Lett. B* **716**, 30–61 (2012).
3. Zyla, P. et al. Review of particle physics. *Prog. Theor. Exp. Phys.* **2020**, 083C01 (2020).
4. Fukuda, Y. et al. Evidence for oscillation of atmospheric neutrinos. *Phys. Rev. Lett.* **81**, 1562–1567 (1998).
5. Ahmad, Q. et al. Direct evidence for neutrino flavor transformation from neutral current interactions in the Sudbury Neutrino Observatory. *Phys. Rev. Lett.* **89**, 011301 (2002).
6. Canetti, L., Drewes, M. & Shaposhnikov, M. Matter and antimatter in the Universe. *New J. Phys.* **14**, 095012 (2012).
7. Abel, C. et al. Measurement of the permanent electric dipole moment of the neutron. *Phys. Rev. Lett.* **124**, 081803 (2020).
8. Hocker, A. et al. TMVA — toolkit for multivariate data analysis. Preprint at *arXiv* https://arxiv.org/abs/physics/0703039 (2007).
9. Deiana, A. M. et al. Applications and techniques for fast machine learning in science. Preprint at *arXiv* https://arxiv.org/abs/2110.13041 (2021).
10. Radovic, A. et al. Machine learning at the energy and intensity frontiers of particle physics. *Nature* **560**, 41–48 (2018).
11. Feickert, M. & Nachman, B. A living review of machine learning for particle physics. Preprint at *arXiv* https://arxiv.org/abs/2102.02770 (2021).
12. Bellagente, M., Butter, A., Kasieczka, G., Plehn, T. & Winterhalder, R. How to GAN away detector effects. *SciPost Phys.* **8**, 070 (2020).
13. Komiske, P., McCormack, W. P. & Nachman, B. Preserving new physics while simultaneously unfolding all observables. Preprint at *arXiv* https://arxiv.org/abs/2105.09923 (2021).
14. Brehmer, J., Kling, F., Espejo, I. & Cranmer, K. MadMiner: machine learning-based inference for particle physics. *Comput. Softw. Big Sci.* **4**, 3 (2020).
15. Brehmer, J., Louppe, G., Pavez, J. & Cranmer, K. Mining gold from implicit models to improve likelihood-free inference. *Proc. Natl Acad. Sci. USA* **117**, 5242–5249 (2020).
16. Brehmer, J., Cranmer, K., Louppe, G. & Pavez, J. Constraining effective field theories with machine learning. *Phys. Rev. Lett.* **121**, 111801 (2018).
17. Brehmer, J., Cranmer, K., Louppe, G. & Pavez, J. A guide to constraining effective field theories with machine learning. *Phys. Rev. D* **98**, 052004 (2018).
18. Grojean, C., Paul, A. & Qian, Z. Resurrecting $b\bar{b}h$ with kinematic shapes. Preprint at *arXiv* https://arxiv.org/abs/2011.13945 (2020).
19. Chatterjee, S., Frohner, N., Lechner, L., Schöfbeck, R. & Schwarz, D. Tree boosting for learning EFT parameters. Preprint at *arXiv* https://arxiv.org/abs/2107.10859 (2021).
20. Chen, S., Glioti, A., Panico, G. & Wulzer, A. Parametrized classifiers for optimal EFT sensitivity. *J. High Energy Phys.* **05**, 247 (2021).
21. Erbin, H. & Krippendorf, S. GANs for generating EFT models. *Phys. Lett. B* **810**, 135798 (2020).
22. Caron, S., Kim, J. S., Rolbiecki, K., Ruiz de Austri, R. & Stienen, B. The BSM-AI project: SUSY-AI – generalizing LHC limits on supersymmetry with machine learning. *Eur. Phys. J. C* **77**, 257 (2017).
23. Bertone, G. et al. Accelerating the BSM interpretation of LHC data with machine learning. *Phys. Dark Univ.* **24**, 100293 (2019).
24. Kronheim, B. S., Kuchera, M. P., Prosper, H. B. & Karbo, A. Bayesian neural networks for fast SUSY predictions. *Phys. Lett. B* **813**, 136041 (2021).
25. Fukushima, K. & Miyake, S. in *Competition and Cooperation in Neural Nets* (eds Amari, S. & Arbib, M. A.) 267–285 (Springer, 1982).
26. LeCun, Y. et al. Handwritten digit recognition with a back-propagation network. *Adv. Neural Inf. Process. Syst.* **2**, 396–404 (1989).
27. de Oliveira, L., Kagan, M., Mackey, L., Nachman, B. & Schwartzman, A. Jet-images — deep learning edition. *J. High Energy Phys.* **07**, 069 (2016).
28. Baldi, P., Bauer, K., Eng, C., Sadowski, P. & Whiteson, D. Jet substructure classification in high-energy physics with deep neural networks. *Phys. Rev. D* **93**, 094034 (2016).
29. Aurisano, A. et al. A convolutional neural network neutrino event classifier. *J. Instrum.* **11**, P09001 (2016).
30. Rumelhart, D. E., Hinton, G. E. & Williams, R. J. Learning representations by back-propagating errors. *Nature* **323**, 533–536 (1986).
31. Hochreiter, S. & Schmidhuber, J. Long short-term memory. *Neural Comput.* **9**, 1735–80 (1997).
32. Guest, D. et al. Jet flavor classification in high-energy physics with deep neural networks. *Phys. Rev. D* **94**, 112002 (2016).

33. Louppe, G., Cho, K., Becot, C. & Cranmer, K. QCD-aware recursive neural networks for jet physics. *J. High Energy Phys.* **01**, 057 (2019).
34. Dolan, M. J. & Ore, A. Equivariant energy flow networks for jet tagging. *Phys. Rev. D* **103**, 074022 (2021).
35. Serviansky, H. et al. Set2graph: learning graphs from sets. Preprint at *arXiv* https://arxiv.org/abs/2002.08772 (2020).
36. Bogatskiy, A. et al. Lorentz group equivariant neural network for particle physics. Preprint at *arXiv* https://arxiv.org/abs/2006.04780 (2020).
37. Shimmin, C. Particle convolution for high energy physics. Preprint at *arXiv* https://arxiv.org/abs/2107.02908 (2021).
38. Zaheer, M. et al. Deep sets. *Adv. Neural Inf. Process. Syst.* **30**, 3391–3401 (2017).
39. Komiske, P. T., Metodiev, E. M. & Thaler, J. Energy flow networks: deep sets for particle jets. *J. High Energy Phys.* **01**, 121 (2019).
40. Henrion, I. et al. Neural message passing for jet physics. in *Proc. Workshop Deep Learning Physical Sciences* (NIPS, 2017).
41. Choma, N. et al. Graph neural networks for IceCube signal classification. Preprint at *arXiv* https://arxiv.org/abs/1809.06166 (2018).
42. Abdughani, M., Ren, J., Wu, L. & Yang, J. M. Probing stop pair production at the LHC with graph neural networks. *J. High Energy Phys.* **08**, 055 (2019).
43. Arjona Martínez, J., Cerri, O., Pierini, M., Spiropulu, M. & Vlimant, J.-R. Pileup mitigation at the Large Hadron Collider with graph neural networks. *Eur. Phys. J. Plus* **134**, 333 (2019).
44. Qu, H. & Gouskos, L. ParticleNet: jet tagging via particle clouds. *Phys. Rev. D* **101**, 056019 (2020).
45. Moreno, E. A. et al. JEDI-net: a jet identification algorithm based on interaction networks. *Eur. Phys. J. C* **80**, 58 (2020).
46. Moreno, E. A. et al. Interaction networks for the identification of boosted $H \to b\bar{b}$ decays. *Phys. Rev. D* **102**, 012010 (2020).
47. Shlomi, J., Battaglia, P. & Vlimant, J.-R. Graph neural networks in particle physics. *Mach. Learn. Sci. Technol.* **2**, 021001 (2021).
48. Cheong, S., Cukierman, A., Nachman, B., Safdari, M. & Schwartzman, A. Parametrizing the detector response with neural networks. *J. Instrum.* **15**, P01030 (2020).
49. Goodfellow, I. J. et al. in *Proc. 27th Int. Conf. Neural Inform. Process. Syst.* Vol. 2 (eds Ghahramani, Z. et al.) 2672–2680 (MIT Press, 2014).
50. Creswell, A. et al. Generative adversarial networks: an overview. *IEEE Signal Process. Mag.* **35**, 53 (2018).
51. Kingma, D. P. & Welling, M. Auto-encoding variational Bayes. Preprint at *arXiv* https://arxiv.org/abs/1312.6114 (2014).
52. Kingma, D. P. & Welling, M. An introduction to variational autoencoders. *Found. Trends Mach. Learn.* **12**, 307 (2019).
53. Rezende, D. J. & Mohamed, S. Variational inference with normalizing flows. *Proc. Mach. Learn. Res.* **37**, 1530–1538 (2015).
54. Kobyzev, I., Prince, S. & Brubaker, M. Normalizing flows: an introduction and review of current methods. *IEEE Trans. Pattern Anal. Mach. Intel.* **43**, 3964–3979 (2021).
55. de Oliveira, L., Paganini, M. & Nachman, B. Learning particle physics by example: location-aware generative adversarial networks for physics synthesis. *Comput. Softw. Big Sci.* **1**, 4 (2017).
56. Mustafa, M. et al. CosmoGAN: creating high-fidelity weak lensing convergence maps using generative adversarial networks. *Comput. Astrophys. Cosmol.* **6**, 1 (2019).
57. ATLAS collaboration. Deep generative models for fast shower simulation in ATLAS. Report ATL-SOFT-PUB-2018-001 (CERN, 2018).
58. Hajer, J., Li, Y.-Y., Liu, T. & Wang, H. Novelty detection meets collider physics. *Phys. Rev. D* **101**, 076015 (2020).
59. Farina, M., Nakai, Y. & Shih, D. Searching for new physics with deep autoencoders. *Phys. Rev. D* **101**, 075021 (2020).
60. Heimel, T., Kasieczka, G., Plehn, T. & Thompson, J. M. QCD or what? *SciPost Phys.* **6**, 030 (2019).
61. Albergo, M. S., Kanwar, G. & Shanahan, P. E. Flow-based generative models for Markov chain Monte Carlo in lattice field theory. *Phys. Rev. D* **100**, 034515 (2019).
62. Gao, C., Höche, S., Isaacson, J., Krause, C. & Schulz, H. Event generation with normalizing flows. *Phys. Rev. D* **101**, 076002 (2020).
63. Gao, C., Isaacson, J. & Krause, C. i-flow: high-dimensional integration and sampling with normalizing flows. *Mach. Learn. Sci. Tech.* **1**, 045023 (2020).
64. Bothmann, E., Janβen, T., Knobbe, M., Schmale, T. & Schumann, S. Exploring phase space with neural importance sampling. *SciPost Phys.* **8**, 069 (2020).
65. Nachman, B. & Shih, D. Anomaly detection with density estimation. *Phys. Rev. D* **101**, 075042 (2020).
66. Zhou, Z.-H. A brief introduction to weakly supervised learning. *Natl Sci. Rev.* **5**, 44–53 (2017).
67. Dery, L. M., Nachman, B., Rubbo, F. & Schwartzman, A. Weakly supervised classification in high energy physics. *J. High Energy Phys.* **05**, 145 (2017).
68. Metodiev, E. M., Nachman, B. & Thaler, J. Classification without labels: learning from mixed samples in high energy physics. *J. High Energy Phys.* **10**, 174 (2017).
69. Cohen, T., Freytsis, M. & Ostdiek, B. (Machine) learning to do more with less. *J. High Energy Phys.* **02**, 034 (2018).
70. Komiske, P. T., Metodiev, E. M., Nachman, B. & Schwartz, M. D. Learning to classify from impure samples with high-dimensional data. *Phys. Rev. D* **98**, 011502 (2018).
71. Knuteson, B. *A Quasi-Model-Independent Search for New High $p_T$ Physics at DØ*. Thesis, Univ. California Berkeley (2000).
72. Abbott, B. et al. Search for new physics in $e\mu X$ data at DØ using Sherlock: a quasi model independent search strategy for new physics. *Phys. Rev. D* **62**, 092004 (2000).
73. Abazov, V. M. et al. A quasi model independent search for new physics at large transverse momentum. *Phys. Rev. D* **64**, 012004 (2001).
74. Abbott, B. et al. A quasi-model-independent search for new high $p_T$ physics at DØ. *Phys. Rev. Lett.* **86**, 3712–3717 (2001).
75. Aaron, F. D. et al. A general search for new phenomena at HERA. *Phys. Lett. B* **674**, 257–268 (2009).
76. Aktas, A. et al. A general search for new phenomena in *ep* scattering at HERA. *Phys. Lett. B* **602**, 14–30 (2004).
77. Cranmer, K. S. *Searching for New Physics: Contributions to LEP and the LHC*. Thesis, Wisconsin Univ. Madison (2005).
78. Aaltonen, T. et al. (CDF Collaboration). Model-independent and quasi-model-independent search for new physics at CDF. *Phys. Rev. D* **78**, 012002 (2008).
79. Aaltonen, T. et al. (CDF Collaboration). Model-independent global search for new high-pT physics at CDF. Preprint at *arXiv* https://arxiv.org/abs/0712.2534 (2007).
80. Aaltonen, T. et al. (CDF Collaboration). Global search for new physics with 2.0 fb$^{-1}$ at CDF. *Phys. Rev. D* **79**, 011101 (2009).
81. CMS Collaboration. MUSiC, a model unspecific search for new physics, in *pp* collisions at $\sqrt{s} = 8$ TeV. Technical Report CMS-PAS-EXO-14-016 (CERN, 2017).
82. CMS Collaboration. Model unspecific search for new physics in *pp* collisions at $\sqrt{s} = 7$ TeV. Technical Report CMS-PAS-EXO-10-021 (CERN, 2011).
83. CMS Collaboration. MUSiC, a model unspecific search for new physics, in *pp* collisions at $\sqrt{s} = 13$ TeV. Technical Report CMS-PAS-EXO-19-008 (CERN, 2020).
84. Sirunyan, A. M. et al. MUSiC: a model-unspecific search for new physics in proton–proton collisions at $\sqrt{s} = 13$ TeV. *Eur. Phys. J. C* **81**, 629 (2021).
85. Aaboud, M. et al. A strategy for a general search for new phenomena using data-derived signal regions and its application within the ATLAS experiment. *Eur. Phys. J. C* **79**, 120 (2019).
86. A general search for new phenomena with the ATLAS detector in *pp* collisions at $\sqrt{s} = 8$ TeV. Report ATLAS-CONF-2014-006 (CERN, 2014).
87. A general search for new phenomena with the ATLAS detector in *pp* collisions at $\sqrt{s} = 7$ TeV. Report ATLAS-CONF-2012-107 (CERN, 2012).
88. Butter, A. et al. The machine learning landscape of top taggers. *SciPost Phys.* **7**, 014 (2019).
89. Abratenko, P. et al. Convolutional neural network for multiple particle identification in the MicroBooNE liquid argon time projection chamber. *Phys. Rev. D* **103**, 092003 (2021).
90. Baldi, P., Sadowski, P. & Whiteson, D. Searching for exotic particles in high-energy physics with deep learning. *Nat. Commun.* **5**, 4308 (2014).
91. Bhimji, W. et al. Deep neural networks for physics analysis on low-level whole-detector data at the LHC. *J. Phys. Conf. Ser.* **1085**, 042034 (2018).
92. Wunsch, S., Jörger, S., Wolf, R. & Quast, G. Optimal statistical inference in the presence of systematic uncertainties using neural network optimization based on binned Poisson likelihoods with nuisance parameters. *Comput. Softw. Big Sci.* **5**, 4 (2021).
93. Elwood, A., Krücker, D. & Shchedrolosiev, M. Direct optimization of the discovery significance in machine learning for new physics searches in particle colliders. *J. Phys. Conf. Ser.* **1525**, 012110 (2020).
94. Xia, L.-G. QBDT, a new boosting decision tree method with systematical uncertainties into training for high energy physics. *Nucl. Instrum. Meth A* **930**, 15–26 (2019).
95. De Castro, P. & Dorigo, T. INFERNO: inference-aware neural optimisation. *Comput. Phys. Commun.* **244**, 170–179 (2019).
96. Charnock, T., Lavaux, G. & Wandelt, B. D. Automatic physical inference with information maximizing neural networks. *Phys. Rev. D* **97**, 083004 (2018).
97. Alsing, J. & Wandelt, B. Nuisance hardened data compression for fast likelihood-free inference. *Mon. Not. R. Astron. Soc.* **488**, 5093–5103 (2019).
98. Heinrich, L. & Simpson, N. pyhf/neos: initial zenodo release. *zenodo* https://doi.org/10.5281/zenodo.3697981 (2020).
99. Dorigo, T. & de Castro, P. Dealing with nuisance parameters using machine learning in high energy physics: a review. Preprint at *arXiv* https://arxiv.org/abs/2007.09121 (2020).
100. Kasieczka, G., Luchmann, M., Otterpohl, F. & Plehn, T. Per-object systematics using deep-learned calibration. *SciPost Phys.* **9**, 089 (2020).
101. Bollweg, S. et al. Deep-learning jets with uncertainties and more. *SciPost Phys.* **8**, 006 (2020).
102. Araz, J. Y. & Spannowsky, M. Combine and conquer: event reconstruction with Bayesian ensemble neural networks. *J. High Energy Phys.* **04**, 296 (2021).
103. Bellagente, M., Haußmann, M., Luchmann, M. & Plehn, T. Understanding event-generation networks via uncertainties. Preprint at *arXiv* https://arxiv.org/abs/2104.04543 (2021).
104. Nachman, B. A guide for deploying deep learning in LHC searches: how to achieve optimality and account for uncertainty. *SciPost Phys.* **8**, 090 (2020).
105. Ghosh, A., Nachman, B. & Whiteson, D. Uncertainty aware learning for high energy physics. Preprint at *arXiv* https://arxiv.org/abs/2105.08742 (2021).
106. Rogozhnikov, A. Reweighting with boosted decision trees. *Proc. Int. Workshop Adv. Comput. Anal. Tech. Phys. Res.* **762**, 012036 (2016).
107. Andreassen, A. & Nachman, B. Neural networks for full phase-space reweighting and parameter tuning. *Phys. Rev. D* **101**, 091901 (2020).
108. Cranmer, K., Pavez, J. & Louppe, G. Approximating likelihood ratios with calibrated discriminative classifiers. Preprint at *arXiv* https://arxiv.org/abs/1506.02169 (2015).
109. Diefenbacher, S. et al. DCTRGAN: improving the precision of generative models with reweighting. *J. Instrum.* **15**, P11004 (2020).
110. Nachman, B. & Thaler, J. Neural conditional reweighting. Preprint at *arXiv* https://arxiv.org/abs/2107.08979 (2021).
111. Clavijo, J. M., Glaysher, P. & Katzy, J. M. Adversarial domain adaptation to reduce sample bias of a high energy physics classifier. Preprint at *arXiv* https://arxiv.org/abs/2005.00568 (2020).
112. Perdue, G. N. et al. Reducing model bias in a deep learning classifier using domain adversarial neural networks in the MINERvA experiment. *J. Instrum.* **13**, P11020 (2018).
113. Lin, J., Bhimji, W. & Nachman, B. Machine learning templates for QCD factorization in the search for physics beyond the standard model. *J. High Energy Phys.* **05**, 181 (2019).
114. Kasieczka, G., Nachman, B., Schwartz, M. D. & Shih, D. Automating the ABCD method with machine learning. *Phys. Rev. D* **103**, 035021 (2021).
115. Mikuni, V., Nachman, B. & Shih, D. Online-compatible unsupervised non-resonant anomaly detection. Preprint at *arXiv* https://arxiv.org/abs/2111.06417 (2021).
116. Blance, A., Spannowsky, M. & Waite, P. Adversarially-trained autoencoders for robust unsupervised new physics searches. *J. High Energy Phys.* **10**, 047 (2019).
117. Englert, C., Galler, P., Harris, P. & Spannowsky, M. Machine learning uncertainties with adversarial neural networks. *Eur. Phys. J. C* **79**, 4 (2019).
118. Louppe, G., Kagan, M. & Cranmer, K. Learning to pivot with adversarial networks. *Adv. Neural Inf. Process. Syst.* **30**, 981–990 (2017).

119. Dolen, J., Harris, P., Marzani, S., Rappoccio, S. & Tran, N. Thinking outside the ROCs: designing decorrelated taggers (DDT) for jet substructure. *J. High Energy Phys.* **05**, 156 (2016).
120. Moult, I., Nachman, B. & Neill, D. Convolved substructure: analytically decorrelating jet substructure observables. *J. High Energy Phys.* **05**, 002 (2018).
121. Stevens, J. & Williams, M. uBoost: a boosting method for producing uniform selection efficiencies from multivariate classifiers. *J. Instrum.* **8**, P12013 (2013).
122. Shimmin, C. et al. Decorrelated jet substructure tagging using adversarial neural networks. *Phys. Rev. D* **96**, 074034 (2017).
123. Bradshaw, L., Mishra, R. K., Mitridate, A. & Ostdiek, B. Mass agnostic jet taggers. *SciPost Phys.* **8**, 011 (2020).
124. ATLAS collaboration. Performance of mass-decorrelated jet substructure observables for hadronic two-body decay tagging in ATLAS. Report ATL-PHYS-PUB-2018-014 (CERN, 2018).
125. Kasieczka, G. & Shih, D. Robust jet classifiers through distance correlation. *Phys. Rev. Lett.* **125**, 122001 (2020).
126. Wunsch, S., Jörger, S., Wolf, R. & Quast, G. Reducing the dependence of the neural network function to systematic uncertainties in the input space. *Comput. Softw. Big Sci.* **4**, 5 (2020).
127. Rogozhnikov, A., Bukva, A., Gligorov, V. V., Ustyuzhanin, A. & Williams, M. New approaches for boosting to uniformity. *J. Instrum.* **10**, T03002 (2015).
128. CMS Collaboration. A deep neural network to search for new long-lived particles decaying to jets. *Mach. Learn. Sci. Technol.* **1**, 035012 (2020).
129. Kitouni, O., Nachman, B., Weisser, C. & Williams, M. Enhancing searches for resonances with machine learning and moment decomposition. Preprint at *arXiv* https://arxiv.org/abs/2010.09745 (2020).
130. Estrade, V., Germain, C., Guyon, I. & Rousseau, D. Systematic aware learning — a case study in high energy physics. *EPJ Web Conf.* **214**, 06024 (2019).
131. Aguilar-Saavedra, J. A., Collins, J. H. & Mishra, R. K. A generic anti-QCD jet tagger. *J. High Energy Phys.* **11**, 163 (2017).
132. Aguilar-Saavedra, J. A., Joaquim, F. R. & Seabra, J. F. Mass unspecific supervised tagging (MUST) for boosted jets. *J. High Energy Phys.* **03**, 012 (2021).
133. Ghosh, A. & Nachman, B. A cautionary tale of decorrelating theory uncertainties. Preprint at *arXiv* https://arxiv.org/abs/2109.08159 (2021).
134. Chouldechova, A. & Roth, A. The frontiers of fairness in machine learning. Preprint at *arXiv* https://arxiv.org/abs/1810.08810 (2018).
135. Mehrabi, N., Morstatter, F., Saxena, N., Lerman, K. & Galstyan, A. A survey on bias and fairness in machine learning. Preprint at *arXiv* https://arxiv.org/abs/1908.09635 (2019).
136. Frate, M., Cranmer, K., Kalia, S., Vandenberg-Rodes, A. & Whiteson, D. Modeling smooth backgrounds and generic localized signals with Gaussian processes. Preprint at *arXiv* https://arxiv.org/abs/1709.05681 (2017).
137. Di Sipio, R., Faucci Giannelli, M., Ketabchi Haghighat, S. & Palazzo, S. DijetGAN: a generative-adversarial network approach for the simulation of QCD dijet events at the LHC. *J. High Energy Phys.* **08**, 110 (2019).
138. Chisholm, A. et al. Non-parametric data-driven background modelling using conditional probabilities. Preprint at *arXiv* https://arxiv.org/abs/2112.00650 (2021).
139. Neyman, J. & Pearson, E. S. On the problem of the most efficient tests of statistical hypotheses. *Phil. Trans. R. Soc. Lond. A* **231**, 289 (1933).
140. Kasieczka, G. et al. The LHC Olympics 2020: a community challenge for anomaly detection in high energy physics. Preprint at *arXiv* https://arxiv.org/abs/2101.08320 (2021).
141. Aarrestad, T. et al. The Dark Machines anomaly score challenge: benchmark data and model independent event classification for the Large Hadron Collider. Preprint at *arXiv* https://arxiv.org/abs/2105.14027 (2021).
142. Hinton, G. E. & Salakhutdinov, R. R. Reducing the dimensionality of data with neural networks. *Science* **313**, 504–507 (2006).
143. Finke, T., Krämer, M., Morandini, A., Mück, A. & Oleksiyuk, I. Autoencoders for unsupervised anomaly detection in high energy physics. Preprint at *arXiv* https://arxiv.org/abs/2104.09051 (2021).
144. Dillon, B. M., Plehn, T., Sauer, C. & Sorrenson, P. Better latent spaces for better autoencoders. Preprint at *arXiv* https://arxiv.org/abs/2104.08291 (2021).
145. Batson, J., Haaf, C. G., Kahn, Y. & Roberts, D. A. Topological obstructions to autoencoding. Preprint at *arXiv* https://arxiv.org/abs/2102.08380 (2021).
146. Fraser, K., Homiller, S., Mishra, R. K., Ostdiek, B. & Schwartz, M. D. Challenges for unsupervised anomaly detection in particle physics. Preprint at *arXiv* https://arxiv.org/abs/2110.06948 (2021).
147. Cerri, O., Nguyen, T. Q., Pierini, M., Spiropulu, M. & Vlimant, J.-R. Variational autoencoders for new physics mining at the Large Hadron Collider. *J. High Energy Phys.* **05**, 036 (2019).
148. Govorkova, E. et al. Autoencoders on FPGAs for real-time, unsupervised new physics detection at 40 MHz at the Large Hadron Collider. Preprint at *arXiv* https://arxiv.org/abs/2108.03986 (2021).
149. Crispim Romão, M., Castro, N. F. & Pedro, R. Finding new physics without learning about it: anomaly detection as a tool for searches at colliders. *Eur. Phys. J. C* **81**, 27 (2021).
150. Dillon, B. M., Faroughy, D. A. & Kamenik, J. F. Uncovering latent jet substructure. *Phys. Rev D.* **100**, 056002 (2019).
151. Caron, S., Hendriks, L. & Verheyen, R. Rare and different: anomaly scores from a combination of likelihood and out-of-distribution models to detect new physics at the LHC. Preprint at *arXiv* https://arxiv.org/abs/2106.10164 (2021).
152. Mikuni, V. & Canelli, F. Unsupervised clustering for collider physics. Preprint at *arXiv* https://arxiv.org/abs/2010.07106v3 (2020).
153. Knapp, O. et al. Adversarially learned anomaly detection on CMS open data: re-discovering the top quark. *Eur. Phys. J. Plus* **136**, 236 (2021).
154. Amram, O. & Suarez, C. M. Tag N' Train: a technique to train improved classifiers on unlabeled data. *J. High Energy Phys.* **01**, 153 (2021).
155. Collins, J. H., Martín-Ramiro, P., Nachman, B. & Shih, D. Comparing weak- and unsupervised methods for resonant anomaly detection. *Eur. Phys. J. C* **81**, 617 (2021).
156. Collins, J. H., Howe, K. & Nachman, B. Anomaly detection for resonant new physics with machine learning. *Phys. Rev. Lett.* **121**, 241803 (2018).
157. Collins, J. H., Howe, K. & Nachman, B. Extending the search for new resonances with machine learning. *Phys. Rev. D* **99**, 014038 (2019).
158. D'Agnolo, R. T. & Wulzer, A. Learning new physics from a machine. *Phys. Rev. D* **99**, 015014 (2019).
159. D'Agnolo, R. T., Grosso, G., Pierini, M., Wulzer, A. & Zanetti, M. Learning multivariate new physics. *Eur. Phys. J. C* **81**, 89 (2021).
160. d'Agnolo, R. T., Grosso, G., Pierini, M., Wulzer, A. & Zanetti, M. Learning new physics from an imperfect machine. Preprint at *arXiv* https://arxiv.org/abs/2111.13633 (2021).
161. Andreassen, A., Nachman, B. & Shih, D. Simulation assisted likelihood-free anomaly detection. *Phys. Rev. D* **101**, 095004 (2020).
162. Benkendorfer, K., Pottier, L. L. & Nachman, B. Simulation-assisted decorrelation for resonant anomaly detection. *Phys. Rev. D* **104**, 035003 (2021).
163. Park, S. E., Rankin, D., Udrescu, S.-M., Yunus, M. & Harris, P. Quasi anomalous knowledge: searching for new physics with embedded knowledge. *J. High Energy Phys.* **21**, 030 (2020).
164. Khosa, C. K. & Sanz, V. Anomaly awareness. Preprint at *arXiv* https://arxiv.org/abs/2007.14462 (2020).
165. Stein, G., Seljak, U. & Dai, B. Unsupervised in-distribution anomaly detection of new physics through conditional density estimation. Preprint at *arXiv* https://arxiv.org/abs/2012.11638 (2020).
166. Hallin, A. et al. Classifying Anomalies THrough Outer Density Estimation (CATHODE). Preprint at *arXiv* https://arxiv.org/abs/2109.00546 (2021).
167. Low, J. F. et al. Boosted decision trees in the CMS level-1 endcap muon trigger. *Proc. Sci.* **2017**, 143 (2017).
168. Gligorov, V. V. & Williams, M. Efficient, reliable and fast high-level triggering using a bonsai boosted decision tree. *J. Instrum.* **8**, P02013 (2013).
169. Aaij, R. et al. The LHCb trigger and its performance in 2011. *J. Instrum.* **8**, P04022 (2013).
170. Duarte, J. et al. Fast inference of deep neural networks in FPGAs for particle physics. *J. Instrum.* **13**, P07027 (2018).
171. Nottbeck, N., Schmitt, C. & Büscher, V. Implementation of high-performance, sub-microsecond deep neural networks on FPGAs for trigger applications. *J. Instrum.* **14**, P09014 (2019).
172. Zabi, A., Berryhill, J. W., Perez, E. & Tapper, A. D. The phase-2 upgrade of the CMS level-1 trigger. Interim Technical Design Report CMS-TDR-017 (CERN, 2020).
173. Summers, S. et al. Fast inference of boosted decision trees in FPGAs for particle physics. *J. Instrum.* **15**, P05026 (2020).
174. Aarrestad, T. et al. Fast convolutional neural networks on FPGAs with hls4ml. *Mach. Learn. Sci. Tech.* **2**, 045015 (2021).
175. Hong, T. M. et al. Nanosecond machine learning event classification with boosted decision trees in FPGA for high energy physics. *J. Instrum.* **16**, P08016 (2021).
176. LHCb Collaboration. LHCb upgrade GPU high level trigger technical design report. CERN-LHCC-2020-006 LHCB-TDR-021 (CERN, 2020).
177. Aaij, R. et al. Allen: a high level trigger on GPUs for LHCb. *Comput. Softw. Big Sci.* **4**, 7 (2020).
178. Chekalina, V. et al. Generative models for fast calorimeter simulation: the LHCb case. *EPJ Web Conf.* **214**, 02034 (2019).
179. ATLAS collaboration. Fast simulation of the ATLAS calorimeter system with generative adversarial networks. Report ATL-SOFT-PUB-2020-006 (CERN, 2020).
180. Aad, G. et al. AtlFast3: the next generation of fast simulation in ATLAS. Preprint at *arXiv* https://arxiv.org/abs/2109.02551 (2021).
181. Aad, G. et al. ATLAS b-jet identification performance and efficiency measurement with $t\bar{t}$ events in pp collisions at $\sqrt{s}$ = 13 TeV. *Eur. Phys. J. C* **79**, 970 (2019).
182. Bols, E., Kieseler, J., Verzetti, M., Stoye, M. & Stakia, A. Jet flavour classification using DeepJet. *J. Instrum.* **15**, P12012 (2020).
183. ATLAS collaboration. Deep sets based neural networks for impact parameter flavour tagging in ATLAS. Report ATL-PHYS-PUB-2020-014 (CERN, 2020).
184. Larkoski, A. J., Moult, I. & Nachman, B. Jet substructure at the Large Hadron Collider: a review of recent advances in theory and machine learning. *Phys. Rep.* **841**, 1–63 (2020).
185. Kogler, R. et al. Jet substructure at the Large Hadron Collider: experimental review. *Rev. Mod. Phys.* **91**, 045003 (2019).
186. Sirunyan, A. M. et al. Identification of heavy, energetic, hadronically decaying particles using machine-learning techniques. *J. Instrum.* **15**, P06005 (2020).
187. Sirunyan, A. M. et al. Search for dark matter particles produced in association with a Higgs boson in proton–proton collisions at $\sqrt{s}$ = 13 TeV. *J. High Energy Phys.* **03**, 025 (2020).
188. CMS Collaboration. Search for resonant Higgs boson pair production in four *b* quark final state using large-area jets in proton–proton collisions at $\sqrt{s}$ = 13 TeV. Technical Report CMS-PAS-B2G-20-004 (CERN, 2021).
189. CMS Collaboration. Search for heavy resonances decaying to a pair of boosted Higgs bosons in final states with leptons and a bottom quark–antiquark pair at $\sqrt{s}$ = 13 TeV. Technical Report CMS-PAS-B2G-20-007 (CERN, 2021).
190. CMS Collaboration. Search for Higgs boson pair production via vector boson fusion with highly Lorentz-boosted Higgs bosons in the four *b* quark final state at $\sqrt{s}$ = 13 TeV. Technical Report CMS-PAS-B2G-21-001 (CERN, 2021).
191. Sirunyan, A. M. et al. Identification of heavy-flavour jets with the CMS detector in *pp* collisions at 13 TeV. *J. Instrum.* **13**, P05011 (2018).
192. Sirunyan, A. M. et al. Search for W′ bosons decaying to a top and a bottom quark at $\sqrt{s}$ = 13 TeV in the hadronic final state. *Phys. Lett. B* **820**, 136535 (2021).
193. ATLAS collaboration. Efficiency corrections for a tagger for boosted $H \to b\bar{b}$ decays in *pp* collisions at $\sqrt{s}$ = 13 TeV with the ATLAS detector. Technical Report ATL-PHYS-PUB-2021-035 (2021).
194. Sirunyan, A. M. et al. A deep neural network to search for new long-lived particles decaying to jets. *Mach. Learn. Sci. Tech.* **1**, 035012 (2020).
195. CMS Collaboration. Identification of highly Lorentz-boosted heavy particles using graph neural networks and new mass decorrelation techniques. Report CMS-DP-2020-002 (CERN, 2020).
196. Tumasyan, A. et al. Search for new particles in events with energetic jets and large missing transverse momentum in proton–proton collisions at $\sqrt{s}$ = 13 TeV. Preprint at *arXiv* https://arxiv.org/abs/2107.13021 (2021).

197. Aaij, R. et al. Search for heavy neutral leptons in $W^+ \to \mu^+\mu^\pm$jet decays. *Eur. Phys. J. C* **81**, 248 (2021).
198. Aad, G. et al. Dijet resonance search with weak supervision using $\sqrt{s} = 13$ TeV *pp* collisions in the ATLAS detector. *Phys. Rev. Lett.* **125**, 131801 (2020).
199. Aaboud, M. et al. Search for pair production of higgsinos in final states with at least three *b*-tagged jets in $\sqrt{s} = 13$ TeV *pp* collisions using the ATLAS detector. *Phys. Rev. D* **98**, 092002 (2018).
200. Aad, G. et al. Search for Higgs boson decays into two new low-mass spin-0 particles in the *4b* channel with the ATLAS detector using *pp* collisions at $\sqrt{s} = 13$ TeV. *Phys. Rev. D* **105**, 012006 (2022).
201. Aad, G. et al. Search for heavy resonances decaying into a pair of *Z* bosons in the $\ell^+\ell^-\ell'^+\ell'^-$ and $\ell^+\ell^-\ell'^+\ell'^-$ final states using 139 fb$^{-1}$ of proton–proton collisions at $\ell^+\ell^-\ell'^+\ell'^-$TeV with the ATLAS detector. *Eur. Phys. J. C* **81**, 332 (2021).
202. Tumasyan, A. et al. Search for a heavy Higgs boson decaying into two lighter Higgs bosons in the $\tau\tau bb$ final state at 13 TeV. Preprint at *arXiv* https://arxiv.org/abs/2106.10361 (2021).
203. Aad, G. et al. Search for Higgs boson decays into *a Z* boson and a light hadronically decaying resonance using 13 TeV *pp* collision data from the ATLAS detector. *Phys. Rev. Lett.* **125**, 221802 (2020).
204. Aad, G. et al. Search for dark matter in events with missing transverse momentum and a Higgs boson decaying into two photons in *pp* collisions at $\sqrt{s} = 13$ TeV with the ATLAS detector. Preprint at *arXiv* https://arxiv.org/abs/2104.13240 (2021).
205. Chen, T. & Guestrin, C. in *Proc. 22nd ACM SIGKDD Int. Conf. Knowledge Discovery Data Mining* 785–794 (ACM, 2016).
206. Bertacchi, V. et al. Track finding at Belle II. *Comput. Phys. Commun.* **259**, 107610 (2021).
207. Abazajian, K. N. et al. Light sterile neutrinos: a white paper. Preprint at *arXiv* https://arxiv.org/abs/1204.5379 (2012).
208. Dentler, M. et al. Updated global analysis of neutrino oscillations in the presence of eV-scale sterile neutrinos. *J. High Energy Phys.* **08**, 010 (2018).
209. Bertuzzo, E., Jana, S., Machado, P. A. N. & Zukanovich Funchal, R. Dark neutrino portal to explain MiniBooNE excess. *Phys. Rev. Lett.* **121**, 241801 (2018).
210. Ballett, P., Pascoli, S. & Ross-Lonergan, M. U(1)′ mediated decays of heavy sterile neutrinos in MiniBooNE. *Phys. Rev. D* **99**, 071701 (2019).
211. Adamson, P. et al. Constraints on large extra dimensions from the MINOS experiment. *Phys. Rev. D* **94**, 111101 (2016).
212. Kostelecky, V. A. & Mewes, M. Lorentz and CPT violation in neutrinos. *Phys. Rev. D* **69**, 016005 (2004).
213. Miranda, O. G. & Nunokawa, H. Non standard neutrino interactions: current status and future prospects. *New J. Phys.* **17**, 095002 (2015).
214. de Gouvêa, A. & Kelly, K. J. Non-standard neutrino interactions at DUNE. *Nucl. Phys. B* **908**, 318–335 (2016).
215. Jwa, Y.-J., Guglielmo, G. D., Carloni, L. P. & Karagiorgi, G. in *2019 New York Sci. Data Summit* (IEEE, 2019).
216. Acciarri, R. et al. A deep-learning based raw waveform region-of-interest finder for the liquid argon time projection chamber. Preprint at *arXiv* https://arxiv.org/abs/2103.06391 (2021).
217. Uboldi, L. et al. Extracting low energy signals from raw LArTPC waveforms using deep learning techniques–a proof of concept. Preprint at *arXiv* https://arxiv.org/abs/2106.09911 (2021).
218. Anker, A. et al. A novel trigger based on neural networks for radio neutrino detectors. *Proc. Sci.* **395**, 1074 (2021).
219. Acero, M. A. et al. Search for active-sterile antineutrino mixing using neutral-current interactions with the NOvA experiment. *Phys. Rev. Lett.* **127**, 201801 (2021).
220. Abratenko, P. et al. Search for an anomalous excess of charged-current quasi-elastic $\nu_e$ interactions with the MicroBooNE experiment using deep-learning-based reconstruction. Preprint at *arXiv* https://arxiv.org/abs/2110.14080 (2021).
221. Baldi, P., Bian, J., Hertel, L. & Li, L. Improved energy reconstruction in NOvA with regression convolutional neural networks. *Phys. Rev. D* **99**, 012011 (2019).
222. Abratenko, P. et al. Wire-cell 3D pattern recognition techniques for neutrino event reconstruction in large LArTPCs: algorithm description and quantitative evaluation with MicroBooNE simulation. Preprint at *arXiv* https://arxiv.org/abs/2110.13961 (2021).
223. Aiello, S. et al. Event reconstruction for KM3NeT/ORCA using convolutional neural networks. *J. Instrum.* **15**, P10005 (2020).
224. Ayres, D. S. et al. The NOvA technical design report. FERMILAB-DESIGN-2007-01 (OSTI, 2007).
225. Psihas, F., Groh, M., Tunnell, C. & Warburton, K. A review on machine learning for neutrino experiments. *Int. J. Mod. Phys. A* **35**, 2043005 (2020).
226. Abi, B. et al. Deep Underground Neutrino Experiment (DUNE), Far Detector Technical Design Report Vol. I: Introduction to DUNE. *J. Instrum.* **15**, T08008 (2020).
227. Acciarri, R. et al. Design and construction of the MicroBooNE detector. *J. Instrum.* **12**, P02017 (2017).
228. Antonello, M. et al. A proposal for a three detector short-baseline neutrino oscillation program in the Fermilab Booster Neutrino Beam. Preprint at *arXiv* https://arxiv.org/abs/1503.01520 (2015).
229. Abi, B. et al. Neutrino interaction classification with a convolutional neural network in the DUNE far detector. *Phys. Rev. D* **102**, 092003 (2020).
230. Liu, J. et al. Deep-learning-based kinematic reconstruction for DUNE. Preprint at *arXiv* https://arxiv.org/abs/2012.06181 (2020).
231. Acciarri, R. et al. Convolutional neural networks applied to neutrino events in a liquid argon time projection chamber. *J. Instrum.* **12**, P03011 (2017).
232. Adams, C. et al. Deep neural network for pixel-level electromagnetic particle identification in the MicroBooNE liquid argon time projection chamber. *Phys. Rev. D* **99**, 092001 (2019).
233. Ronneberger, O., Fischer, P. & Brox, T. U-net: convolutional networks for biomedical image segmentation. Preprint at *arXiv* https://arxiv.org/abs/1505.04597 (2015).
234. Abratenko, P. et al. Semantic segmentation with a sparse convolutional neural network for event reconstruction in MicroBooNE. *Phys. Rev. D* **103**, 052012 (2021).
235. Dominé, L. & Terao, K. Scalable deep convolutional neural networks for sparse, locally dense liquid argon time projection chamber data. *Phys. Rev. D* **102**, 012005 (2020).
236. Acciarri, R. et al. Cosmic background removal with deep neural networks in SBND. Preprint at *arXiv* https://arxiv.org/abs/2012.01301 (2020).
237. Drielsma, F., Terao, K., Dominé, L. & Koh, D. H. Scalable, end-to-end, deep-learning-based data reconstruction chain for particle imaging detectors. Preprint at *arXiv* https://arxiv.org/abs/2102.01033 (2021).
238. Dominé, L. & Terao, K. Point proposal network for reconstructing 3D particle positions with sub-pixel precision in liquid argon time projection chambers. Preprint at *arXiv* https://arxiv.org/abs/2006.14745 (2020).
239. Koh, D. H. et al. Scalable, proposal-free instance segmentation network for 3d pixel clustering and particle trajectory reconstruction in liquid argon time projection chambers. Preprint at *arXiv* https://arxiv.org/abs/2007.03083 (2020).
240. Drielsma, F. et al. Clustering of electromagnetic showers and particle interactions with graph neural networks in liquid argon time projection chambers. *Phys. Rev. D* **104**, 072004 (2021).
241. Adams, C., Terao, K. & Wongjirad, T. PILArNet: public dataset for particle imaging liquid argon detectors in high energy physics. Preprint at *arXiv* https://arxiv.org/abs/2006.01993 (2020).
242. Psihas, F. The convolutional visual network for identification and reconstruction of NOvA events. *J. Phys. Conf. Ser.* **898**, 072053 (2017).
243. Gando, A. et al. Search for Majorana neutrinos near the inverted mass hierarchy region with KamLAND-Zen. *Phys. Rev. Lett.* **117**, 082503 (2016); addendum **117**, 109903 (2016).
244. Racah, E. et al. Revealing fundamental physics from the Daya Bay neutrino experiment using deep neural networks. Preprint at *arXiv* https://arxiv.org/abs/1601.07621 (2016).
245. Choma, N. et al. Graph neural networks for IceCube signal classification. Preprint at *arXiv* https://arxiv.org/abs/1809.06166 (2018).
246. Abbasi, R. et al. Reconstruction of neutrino events in IceCube using graph neural networks. *Proc. Sci.* **395**, 1044 (2021).
247. Abi, B. et al. Deep Underground Neutrino Experiment (DUNE), Far Detector Technical Design Report, Vol. III: DUNE far detector technical coordination. *J. Instrum.* **15**, T08009 (2020).
248. Wang, M. et al. GPU-accelerated machine learning inference as a service for computing in neutrino experiments. *Front. Big Data* **3**, 604083 (2021).
249. Akerib, D. S. et al. Improving sensitivity to low-mass dark matter in LUX using a novel electrode background mitigation technique. *Phys. Rev. D* **104**, 012011 (2021).
250. Akerib, D. S. et al. Constraints on effective field theory couplings using 311.2 days of LUX data. Preprint at *arXiv* https://arxiv.org/abs/2102.06998 (2021).
251. Rossiter, P. *Background Mitigation in Dual Phase Xenon Time Projection Chambers*. Thesis, Sheffield Univ. (2021).
252. Aprile, E. et al. Search for coherent elastic scattering of solar $^8$B neutrinos in the XENON1T dark matter experiment. *Phys. Rev. Lett.* **126**, 091301 (2021).
253. Agnese, R. et al. Search for low-mass dark matter with CDMSlite using a profile likelihood fit. *Phys. Rev. D* **99**, 062001 (2019).
254. Adhikari, G. et al. Lowering the energy threshold in COSINE-100 dark matter searches. *Astropart. Phys.* **130**, 102581 (2021).
255. Albert, J. B. et al. Search for $2\nu\beta\beta$ decay of $^{136}$Xe to the $0_1^+$ excited state of $^{136}$Ba with EXO-200. *Phys. Rev. C* **93**, 035501 (2016).
256. Albert, J. B. et al. Search for neutrinoless double-beta decay with the upgraded EXO-200 detector. *Phys. Rev. Lett.* **120**, 072701 (2018).
257. Anton, G. et al. Search for neutrinoless double-$\beta$ decay with the complete EXO-200 dataset. *Phys. Rev. Lett.* **123**, 161802 (2019).
258. Yu, T. C. Template-free pulse height estimation of microcalorimeter responses with PCA. Preprint at *arXiv* https://arxiv.org/abs/1910.14261 (2019).
259. Wagner, F. *Machine Learning Methods for the Raw Data Analysis of Cryogenic Dark Matter Experiments*. Thesis, TU Wien (2020).
260. Holl, P. et al. Deep learning based pulse shape discrimination for germanium detectors. *Eur. Phys. J. C* **79**, 450 (2019).
261. Matusch, B. et al. Developing a bubble chamber particle discriminator using semi-supervised learning. Preprint at *arXiv* https://arxiv.org/abs/1811.11308 (2018).
262. Matusch, B. & Cao, G. Particle identification using semi-supervised learning in the PICO-60 dark matter detector. *J. Phys. Conf. Ser.* **1525**, 012085 (2020).
263. Mühlmann, C. *Pulse-Shape Discrimination with Deep Learning in CRESST*. Thesis, TU Wien (2019).
264. Ai, P., Wang, D., Huang, G. & Sun, X. Three-dimensional convolutional neural networks for neutrinoless double-beta decay signal/background discrimination in high-pressure gaseous time projection chamber. *J. Instrum.* **13**, P08015 (2018).
265. Renner, J. et al. Background rejection in NEXT using deep neural networks. *J. Instrum.* **12**, T01004 (2017).
266. Kekic, M. et al. Demonstration of background rejection using deep convolutional neural networks in the NEXT experiment. *J. High Energy Phys.* **01**, 189 (2021).
267. Li, Z. et al. Simulation of charge readout with segmented tiles in nEXO. *J. Instrum.* **14**, P09020 (2019).
268. Adhikari, G. et al. nEXO: neutrinoless double beta decay search beyond $10^{28}$ year half-life sensitivity. Preprint at *arXiv* https://arxiv.org/abs/2106.16243 (2021).
269. Qiao, H. et al. Signal-background discrimination with convolutional neural networks in the PandaX-III experiment using MC simulation. *Sci. China Phys. Mech. Astron.* **61**, 101007 (2018).
270. Li, A., Elagin, A., Fraker, S., Grant, C. & Winslow, L. Suppression of cosmic muon spallation backgrounds in liquid scintillator detectors using convolutional neural networks. *Nucl. Instrum. Meth. A* **947**, 162604 (2019).
271. Golovatiuk, A., Ustyuzhanin, A., Alexandrov, A. & De Lellis, G. Deep learning for direct dark matter search with nuclear emulsions. Preprint at *arXiv* https://arxiv.org/abs/2106.11995 (2021).
272. Simola, U., Pelssers, B., Barge, D., Conrad, J. & Corander, J. Machine learning accelerated likelihood-free event reconstruction in dark matter direct detection. *J. Instrum.* **14**, P03004 (2019).
273. Delaquis, S. et al. Deep neural networks for energy and position reconstruction in EXO-200. *J. Instrum.* **13**, P08023 (2018).
274. Aprile, E. et al. XENON1T dark matter data analysis: signal reconstruction, calibration and event selection. *Phys. Rev. D* **100**, 052014 (2019).

275. Goicoechea-Casanueva, V., Kish, A. & Maricic, J. Event vertex reconstruction with deep neural networks for the DarkSide-20k experiment. *EPJ Web Conf.* **251**, 03029 (2021).
276. Grobov, A. & Ilyasov, A. Convolutional neural network approach to event position reconstruction in DarkSide-50 experiment. *J. Phys. Conf. Ser.* **1690**, 012013 (2020).
277. Ashtari Esfahani, A. et al. Cyclotron radiation emission spectroscopy signal classification with machine learning in Project 8. *New J. Phys.* **22**, 033004 (2020).
278. Abadi, M. et al. TensorFlow: large-scale machine learning on heterogeneous systems. Preprint at *arXiv* https://arxiv.org/abs/1603.04467 (2016).
279. Paszke, A. et al. Pytorch: an imperative style, high-performance deep learning library. *Adv. Neural Inf. Process. Syst.* **32**, 8024–8035 (2019).
280. Lindegren, L. et al. Gaia Data Release 2. The astrometric solution. *Astron. Astrophys.* **616**, A2 (2018).
281. Abbott, B. P. et al. LIGO: the Laser Interferometer Gravitational-wave Observatory. *Rep. Prog. Phys.* **72**, 076901 (2009).
282. Ivezić, Ž. et al. LSST: from science drivers to reference design and anticipated data products. *Astrophys. J.* **873**, 111 (2019).
283. Weltman, A. et al. Fundamental physics with the Square Kilometre Array. *Publ. Astron. Soc. Aust.* **37**, e002 (2020).
284. Stein, G. georgestein/ml-in-cosmology: machine learning in cosmology. *zenodo* https://doi.org/10.5281/zenodo.4024768 (2020).

**Acknowledgements**
S.K. and B.N. are supported by the US Department of Energy (DOE) Office of Science under contract DE-AC02-05CH11231. G. Kasieczka acknowledges the support of the Deutsche Forschungsgemeinschaft (DFG, German Research Foundation) under Germany's Excellence Strategy — EXC 2121 'Quantum Universe' — 390833306. The work of D.S. was supported by DOE grant DOE-SC0010008. G. Karagiorgi is supported by the US National Science Foundation under grant no. PHY-1753228.

**Author contributions**
The authors contributed equally to all aspects of the article.

**Competing interests**
The authors declare no competing interests.

**Peer review information**
*Nature Reviews Physics* thanks the anonymous reviewers for their contribution to the peer review of this work.

**Publisher's note**
Springer Nature remains neutral with regard to jurisdictional claims in published maps and institutional affiliations.

© Springer Nature Limited 2022